A Letters Journal Exploring the Frontiers of Physics

March 2009

EPL, **85** (2009) 60002
doi: 10.1209/0295-5075/85/60002

www.epljournal.org

The behavior of bouncing disks and pizza tossing

K.-C. Liu, J. Friend[(a)] and L. Yeo

MicroNanophysics Research Laboratory, Department of Mechanical Engineering, Monash University Melbourne, Victoria 3800, Australia

received 26 January 2009; accepted in final form 20 February 2009
published online 26 March 2009

PACS 05.45.-a – Nonlinear dynamics and chaos
PACS 84.60.-h – Direct energy conversion and storage
PACS 43.38.Fx – Piezoelectric and ferroelectric transducers

Abstract – We investigate the dynamics of a disk bouncing on a vibrating platform – a variation of the classic bouncing ball problem – that captures the physics of pizza tossing and the operation of certain standing-wave ultrasonic motors (SWUMs). The system's dynamics explains why certain tossing motions are used by dough-toss performers for different tricks: a helical trajectory is used in *single tosses* because it maximizes energy efficiency and the dough's airborne rotational speed, a semi-elliptical motion is used in *multiple tosses* because it is easier for maintaining dough rotation at the maximum rotational speed. The system's bifurcation diagram and basins of attraction also informs SWUM designers about the optimal design for high speed and minimal sensitivity to perturbation.

Introduction. – Like many nonlinear dynamical systems, the equations governing a ball bouncing on a vibrating platform is simple to describe, yet complex in its behaviour. The system displays a range of intriguing phenomena including noise-sensitive hysteresis loops [1], period doubling route to chaos, and eventually periodic orbits known variously as the "sticking solution", or "complete chattering" [2,3]. The system's physical simplicity and rich nonlinear behaviour have motivated a variety of applications, ranging from its use as a pedagogical tool [4] to the dynamics of granular gases [5] and high-energy ball milling [6].

A particularly interesting extension of the system consists of a *disk* with angular α and linear x displacement, bouncing on a vibrating platform with combined angular β and linear oscillation s described by

$$\beta(t) = \Phi \sin(\omega t + \theta) \qquad \text{and} \qquad s(t) = A \sin(\omega t). \tag{1}$$

The rotational degree of freedom opens up a whole new set of phenomena; whereas the reciprocal platform motion with finite restitution gives rise to an average vertical velocity of zero, the stick-slip rotation while the disk and platform are in contact and the impulsive frictional torque imparted at each collision can produce a continuous rotary motion.

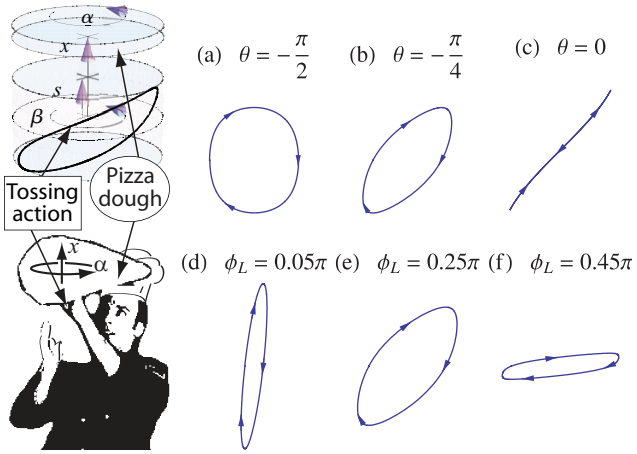

Fig. 1: (Color online) A family of basic dough tossing motion: the trajectory traced by the hand as we vary: (a)–(c) θ at $\phi_L = \pi/4$, and (d)–(f) $L = \tan(\phi_L)$ at $\theta = -\pi/4$.

This process of motion transfer is intimately related to pizza tossing and the stator-rotor interaction in a class of standing-wave ultrasonic motors (SWUMs) [7,8]. The trajectories traced by a dough-tossing hand and the stator motion in SWUMs closely resemble paths described by eq. (1); fig. 1 shows a family of such paths as amplitude ratio $L = a_e\Phi/A = \tan\phi_L$ and phase lag θ are varied (a_e is the effective frictional radius).

[(a)] E-mail: james.friend@eng.monash.edu.au

In general, when a pizza dough is tossed from rest, the tossing motion traces a helical trajectory resembling fig. 1(c); the dough is then caught upon its descent, allowed to come to rest, and the process is repeated (see video footage of pizza tossing online: single tosses [1], multiple tosses [9]). We conjecture that the tossing motion naturally adopted by performers provide certain advantages in terms of effort, speed, and ease of handling; thus, in light of the link between pizza tossing and SWUM, the techniques used in the former could provide insights into the optimal design of SWUMs. In this paper, we investigate the basic pizza toss through the bouncing disk model, considering in detail the effect of the tossing motion on the energy efficiency and rotation speed of an idealized dough ball. Note that our focus is on pizza tossing as a method for imparting rotary motion rather than dough shaping; since the typical rate of dough deformation is low (the diameter increases $\sim 3\%$ per toss in the second video of [9]), dough plasticity only has a minor effect on the dynamics and is thus ignored. Furthermore, we treat SWUMs that share only a small area of contact between the stator and rotor, a large majority of such motors. It is important to note that if the area of contact between the rotor and stator is significant and the frequency of oscillation of the stator is only modestly ultrasonic, the presence of air or another fluid in the gap between the two can influence the dynamics of the combined system. Indeed, one may exploit the small fluid gap in *near-field acoustic levitation* to form a variety of fascinating levitation [10] and propulsion [11,12] phenomena. Our motors, as all other SWUMs purposely designed to operate with friction in contact that we are aware of, do not encounter significant acoustic levitation forces.

The bouncing disk model. – Following the traditional approach to the bouncing-ball problem [3], collisions have zero duration and are characterized by a speed independent coefficient of restitution ϵ. For the rotary component, we assume that the contact pressure is uniform and the torque is transmitted via Coulomb friction with a constant cofficient of friction μ and an effective contact radius a_e. The governing equations for the motion of the disk are then

$$m\ddot{x} = -mg + N + \sum_{n=1}^{\infty} \hat{F}_n \delta(t - t_n), \quad \text{and} \tag{2a}$$

$$m a_g^2 \ddot{\alpha} = -\mu a_e N \mathrm{sgn}(\dot{\alpha} - \dot{\beta}) + \sum_{n=1}^{\infty} -\hat{H}_n \delta(t - t_n), \tag{2b}$$

where N is the normal contact force, $\hat{F}_n$ and $\hat{H}_n$ are the linear and angular impulses at t_n from the disk's n-th collision with the platform, δ is the Dirac delta-function, m is the disk's mass, and a_g is the radius of gyration.

[1]Video footage (`toss-footage.mov`) of single pizza tosses performed by Noah Elhage, captured on 3 October, 2007, camera operated by Kuang-Chen Liu.

Due to the discontinuities introduced by separation ($N \not< 0$), impulsive force ($\hat{F}_n$, $\hat{H}_n$), and friction force $-\mu a_e N \mathrm{sgn}(\dot{\alpha} - \dot{\beta})$, the disk described by eqs. (2) experiences four distinct phases: 1) parabolic flight, 2) impact, 3) sticking contact, and 4) sliding contact, each of which has an analytical solution. Thus the disc's motion is solved if the correct sequence and durations of the phases are found. We do this through a phase stepping alogrithm, in which the final condition of the current phase and the identity of the succeeding phase are determined at each step.

Single tosses. – First, we apply our model to determine the best motion for tossing a dough from rest as θ and L are varied. Three quantities are used as performance measures for the different tossing motions: 1) the airborne rotational speed reached by the pizza dough $\dot{\alpha}_f$, 2) speed ratio ν – airborne speed $\dot{\alpha}_f$ over maximum platform speed $\omega\Phi$, and 3) energy efficiency η – ratio of the rotational kinetic energy gained by the disk ΔE_r over the total energy input from the platform E_{in}.

While varying the amplitude ratio L, we keep the arc length of the helical dough tossing trajectory $c = \sqrt{A^2 + (a_e\Phi)^2}$ constant; since $L = \tan(\phi_L) = a_e\Phi/A$, we have $(a_e\Phi, A) = c(\sin\phi_L, \cos\phi_L)$, and by varying ϕ_L between 0 and $\pi/2$ all possible L from 0 to ∞ are considered. The parameters for this investigation are based on a video of pizza tossing recorded at a local pizza shop (see footnote [1]). The arc length of the helical pizza tossing action $2c$ is estimated to be 50 cm; the peak velocity of the toss ωc is on the order of 5 m/s, thus we choose $\omega = 6\pi\,\mathrm{rad/s} = 3\,\mathrm{Hz}$; the diameter of a typical pizza is $d = 30\,\mathrm{cm}$ and is used to determine the radius of friction and gyration ($a_e = 0.4d$ and $a_g = d/2\sqrt{2}$); the coefficient of friction between skin and dough is estimated to be $\mu = 0.6$ by a simple experiment (baked bread begins to slip from a lightly floured hand at $\sim 30^\circ$ slope); and $g = 10\,\mathrm{m/s^2}$. The coefficient of restitution does not play a role in the single-toss mode since the dough is allowed to come to rest before the next toss is performed. The process can be considered as a chain of single tosses with the pizza dough initially resting at the lowest point of the tossing motion (*i.e.* $t_0 = 3T/4 = 3\pi/2\omega$).

Contour plots of the airborne speed $\dot{\alpha}_f$, speed ratio ν and energy efficiency η are shown in fig. 2 with extremal points marked with crosses. The optimal parameters are $\theta = 0$ or π, and $\phi_L = 0.248\pi$ ($L \approx 1$), where the maximum airborne speed $\dot{\alpha}_f = 27.1\,\mathrm{rpm}$ and energy efficiency $\eta = 0.519$ are reached (the speed ratio at these points $|\nu| = 0.983$ is only slightly less than the maximum of 0.995). The optimal motion predicted by our bouncing disk model is precisely the helical motion of fig. 1(c) seen in actual pizza tossing.

Though our model is simple, the essential physics of the torque transfer process in pizza tossing are included so that we can say qualitatively that the optimal motion for tossing a pizza dough initially at rest is the helical motion employed by practising pizza chefs. Supporting

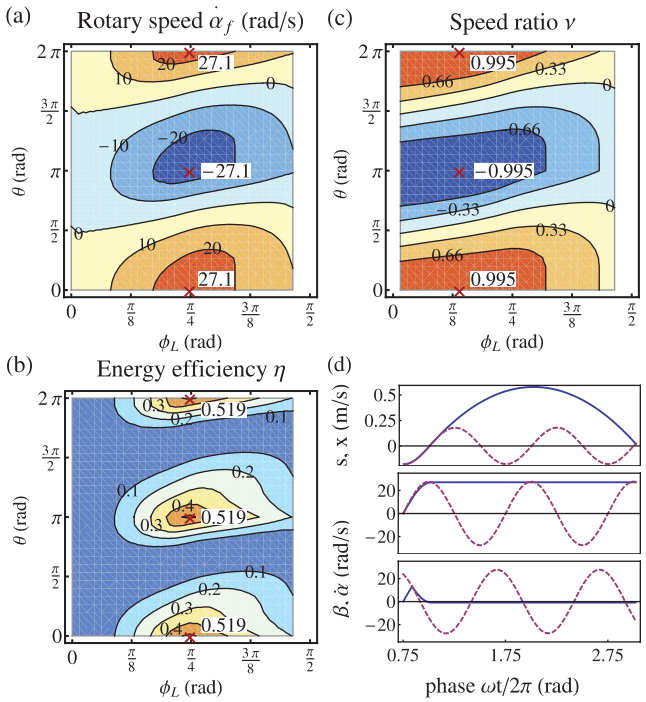

Fig. 2: (Color online) (a)–(c) The performance of different pizza tossing techniques when phase lag θ and amplitude ratio ϕ_L are varied. (d) Details of two different tossing motions (red dashed curve) and the resulting pizza dough trajectory (blue solid curve): first row: the common axial displacement when $\phi_L = 0.25\pi$, second and third rows: angular velocity for $\theta = 0$ and $\theta = 0.5\pi$.

our use of the bouncing disk model is the fact that our simulation – with parameters based on actual pizza tossing motion – gave predictions of the same order of magnitude as the actual motion: the average airborne angular speed of the first four pizza tosses in the video footage `toss-footage.mov` (see footnote [1]) is 13.9 ± 1.41 rad/s compared to the maximum angular speed of 27.1 rad/s from the simulations.

The detailed trajectory of the disc when $\theta = 0$ and $\phi_L = \pi/4$ (see fig. 2(d)) illustrates why it is the optimal motion for single tosses. Beginning with the dough at rest, torque is transferred via sliding or static friction. Given a sufficient static friction limit, the airborne rotation speed of the dough will match the rotation speed of the tossing motion at the point of separation (when $\ddot{s}$ falls below $-g$). Describing the timing of the tossing motion in terms of the nondimensional phase $\tau = \omega t$, the point of separation τ_{sep} and the point of maximum platform rotation speed $\tau_{\max|\dot{\beta}|}$ are given by

$$\tau_{\text{sep}} = \sin^{-1}(1/\pi\Gamma), \quad \text{and} \quad \tau_{\max|\dot{\beta}|} = -\theta + n\pi, \qquad (3)$$

where $n = 0, 1\ldots$, and $\Gamma = A\omega^2/\pi g$ is the axial forcing parameter. If there is no slip, the maximum $|\dot{\alpha}_f|$ is obtained for a specific amplitude ratio if τ_{sep} coincides with $\tau_{\max|\dot{\beta}|}$. Since $\tau_{\text{sep}} \approx 0$ when ϕ_L is low for minimizing slip, the optimal phase lag $\theta = -\tau_{\max|\dot{\beta}|} = -\tau_{\text{sep}} \approx 0$. In comparison, elliptical motions with phase lag of $\theta = \pm\pi/2$ reaches zero rotational speed when the dough is released, resulting in tosses with poor efficiency and low rotational speed. Note that the optimal amplitude ratio $\phi_L \approx \pi/4$ results from the compromise between the goal of minimizing slip (which favours lower ϕ_L) and the goal of maximizing $|\dot{\beta}|$ (which favours higher ϕ_L).

Multiple tosses. – So far we have ignored the coefficient of restitution and considered only single tosses where the effect of collisions can be ignored. However, impact and the associated nonlinear phenomena becomes important if the rotation of the dough is maintained over multiple tosses. Indeed such acts are regularly carried out by advanced dough-toss performers [9], and are the norm in the stator-rotor interaction of SWUMs.

In contrast to single tosses, the motion employed by dough-toss performers to maintain dough rotation over multiple tosses is generally a semi-elliptical trajectory resembling fig. 1(b). Similarly, SWUM researchers believe that the optimal stator motion to spin the rotor is an elliptical motion (fig. 1(a)). In this half of our letter, we investigate the differences in the preferred tossing motion for single and multiple tosses.

For the multiple-toss mode, all or most of the angular momentum transfer from the stator to the rotor is impulsive. If the angular momentum transferred to the rotor at each collision is the maximum possible value for a given coefficient of friction μ and stator angular oscillation $a_e\Phi$, then the rotor would eventually rotate with the maximum angular velocity of $\omega\Phi$; at steady state, the maximum possible angular impulse is zero (all other possible impulses are negative). In terms of a "next collision" map, this suggests that the optimal toss corresponds to a period-1 orbit where the phase at impact τ_{imp} coincides with $\tau_{\max|\dot{\beta}|}$. The main reason SWUM researchers believe that the optimal stator motions are elliptical is that they assume contact always occurs as the stator peaks in its axial displacement ($\tau \approx \pi/2$); thus an elliptical stator motion with $\theta = -\tau_{\max|\dot{\beta}|} = -\pi/2$ would be optimal.

We formulate a next collision map through our computational model of the bouncing disk system and select as state variables the relative axial collision velocity $w_A = \dot{x} - \dot{s}$, the relative angular collision velocity $w_T = \dot{\alpha} - \dot{\beta}$, and the phase at impact $\tau_{\text{imp}} = \omega t_{\text{imp}}$. The nondimensionalised form of the map has four parameters: Γ, ϵ, θ as previously defined, and an angular forcing parameter $\Gamma_T = a_g^2\Phi\omega^2/a_e\pi g\mu$ which can be interpreted as the ratio of angular inertia torque to frictional torque.

In the present variant of the bouncing-ball problem, the frictional coupling is asymmetric: the angular component is affected by the axial component but not vice versa. The vertical motion of our bouncing disk (*pizza*) system is thus identical to the traditional bouncing ball system, and the bifurcation diagram for the τ_{imp} shown in fig. 3(a) is essentialy the same as Tufillaro's [2]. The plot was produced

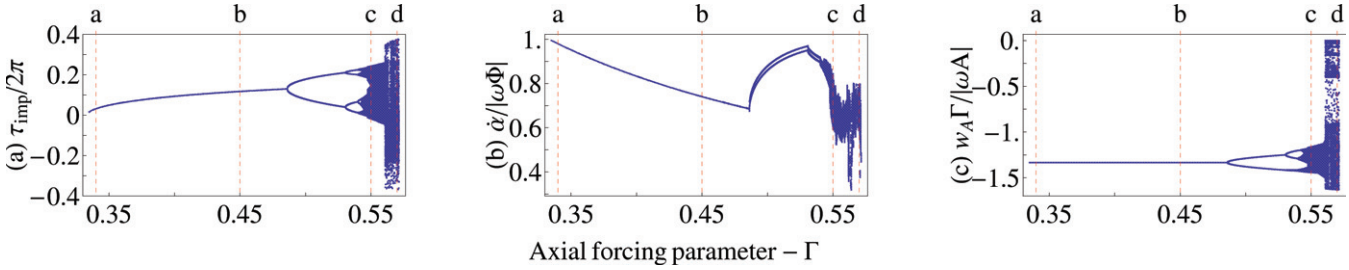

Fig. 3: (Color online) (a) Bifurcation plot of $\tau_{\rm imp}$ showing a period-doubling route to chaos ($\epsilon = 0, 5$). (b) Angular speed of the orbits if $\theta = 0$ and $\Gamma_T = 100$. (c) The relative collision speed. Note that ϕ_L is not fixed. The basins of attraction for points a–d are shown in fig. 4. The first 4 bifurcation points are 0.486, 0.531, 0.5402, 0.5421, which gives rise to the following ratios 4.891, 4.842, 4.75 ..., evidently approaching the Feigenbaum constant 4.669 .... .

for $\epsilon = 0.5$ by "following" the period-1 attractor [13] at $\Gamma = 0.335$, which undergoes a period-doubling route to chaos as Γ is increased.

For period-1 orbits, the dough's steady-state rotational velocity $\dot{\alpha}_{\rm p1,ss}$ matches the platform rotation $\dot{\beta}$ at impact,

$$\dot{\alpha}_{\rm p1,ss} = \dot{\beta}(t_{\rm imp}) = \omega\Phi\cos(\tau_{\rm imp} + \theta), \qquad (4)$$

hence the steady-state rotational speed is maximized if $\theta = -\tau_{\rm imp}$. The period-1 orbits in fig. 3 begins with $\tau_{\rm imp} = 0$ at $\Gamma = 1/3$ and gradually shifts towards $\tau_{\rm imp}/2\pi = 0.13$ at $\Gamma = 0.486$ where period-2 bifurcation occurs; this means that the stator motion needed achieve $\max|\dot{\alpha}_{\rm p1,ss}|$ varies from a helical to a semi-elliptical trajectory depending on Γ. For example, it follows from eq. (4) that a helical trajectory $\theta = 0$ would result in $\max|\dot{\alpha}_{\rm p1,ss}|$ if $\Gamma = 1/3$; this is shown in fig. 3(b) where the rotational component $\dot{\alpha}/|\omega\Phi|$ of a system with $\theta = 0$ and $\Gamma_T = 100$ starts from the maximum of $\dot{\alpha}/|\omega\Phi| = 1$ when $\tau_{\rm imp} = 0$ at $\Gamma = 1/3$, and decreases as $\tau_{\rm imp}$ shifts away from $\theta = 0$.

After the period-2 bifurcation, eq. (4) no longer applies; the steady-state orbit oscillates between two states as the collisions alternate between the large-$|w_A|$ lower branch and the small-$|w_A|$ upper branch (see fig. 3(c)). The steady-state rotational speed is biased towards $\dot{\beta}$ of the lower branch due its higher axial impact speed $|w_A|$. Thus, as the lower branch shifts back towards $\tau = 0$, the average rotational speed rises until the peak at the period-4 bifurcation. Beyond the period-4 bifurcation, and into the chaotic and chattering regime, the average $\dot{\alpha}$ is significantly reduced due to a large proportion of the impacts occuring with lower $\dot{\beta}$.

Note that by choosing the right phase lag ($\theta = -\tau_{\rm imp}$), we can achieve the maximum steady-state rotational speed if Γ is in the period-1 region ($0.333 < \Gamma < 0.486$). Thus the elliptical motion is not the best stator trajectory for the reasons that SWUM researchers have assumed. Nevertheless, a semi-elliptical trajectory still appears to be preferred in multiple pizza tosses, based on video footages of multiple tosses [9]. We explain this by considering if there are advantages for choosing a particular Γ for

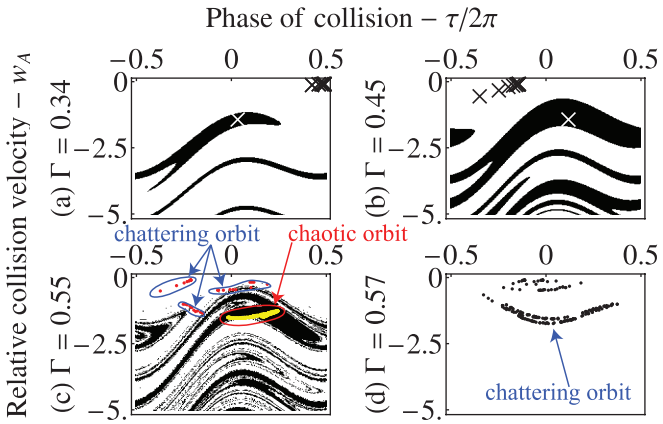

Fig. 4: (Color online) The basins of attraction for $\Gamma = 0.34, 0.45, 0.55, 0.60$. In the first three plots the white region is the basin of the chattering orbit marked by black "×'s" or red dots; the black region is the basin of the attractors marked by white "×'s" or yellow dots. In the fourth plot, the whole region is in the basin of the attractor marked by the black dots.

tossing pizzas. Intuitively, the lowest Γ appears to be energetically preferable. However, fig. 4 shows that the basin of attraction for the period-1 orbit only covers 11.6% of the shown phase space at $\Gamma = 0.34$ and widens to 34.7% at $\Gamma = 0.45$. A wide basin of attraction implies a wider margin of variability allowed in the performance. Thus it would be "easier" to maintain a period-1 orbit for $\Gamma \approx 0.486$, where the optimal phase lag is $\theta = -0.26\pi$, which is a semi-elliptical trajectory.

Co-existing with the period-1 attractors are high-period, chattering orbits marked by black crosses. These orbits can be categorized in the same class as the single tosses: following a high toss, the dough approaches rest during the chattering phase and the process is repeated. Their wide basins suggests why the single toss is so much easier to perform than the multiple toss. The fact that period-1 basins do not cross the $w_A = 0$ axis implies that period-1 orbits cannot occur for a dough initially at rest if the tossing motion purely follows eq. (1). This explains why performers use the helical motion for the first toss and change in the subsequent tosses to a semi-elliptical motion.

The chaotic and chattering region of fig. 3 informs pizza tossers of the forcing parameters that should be avoided, and furthermore provides insights into improving the operation of SWUMs. The fractal nature of the basin boundary for the attractors in $\Gamma = 0.55$ implies a sensitive dependence on initial condition, and the motors should be designed operate outside the chaotic regime. The suitability of the chattering regime for SWUM operation is less obvious. In fig. 3(a), the start of the chattering regime is marked by a sudden widening of the phase space explored by the orbits following the chaotic regime. The strange attractor of the chaotic orbits merges with the chattering orbit and the basin of attraction appears to fill the entire phase space. The wide basin suggests that if a SWUM can be designed to operate in the chattering regime, it would be able to withstand the most disturbance. However, it would be difficult to improve the rotational speed due to the large region of the phase space visited by the orbit.

Conclusion. – Pizza tossing and SWUMs share a common mechanism for converting reciprocal input into continuous rotary motion. In order to better understand this motion transfer process, we have formulated a bouncing-disk model that captures its key features: impact, separation and stick-slip frictional torque. Of the two basic pizza tossing modes that we have investigated, we found that the preferred tossing motion optimizes different performance measures: the helical trajectory used in single tosses maximizes rotation speed and efficiency, and the semi-elliptical motion used in multiple tosses is related to the ease of maintaining the pizza in the period-1 orbits that are required for maximum steady-state speed. Further investigation of the system on the effects of parameters such as ϵ and Γ_T will prove fruitful for the understanding and design of SWUMs.

REFERENCES

[1] Pierański P., *Phys. Rev. A*, **37** (1988) 1782.
[2] Tufillaro N. B., *Phys. Rev. E*, **50** (1994) 4509.
[3] Luck J. M. and Mehta A., *Phys. Rev. E*, **48** (1993) 3988.
[4] Tufillaro N. B. and Albano A. M., *Am. J. Phys.*, **54** (1986) 939.
[5] Géminard J.-C. and Laroche C., *Phys. Rev. E*, **68** (2003) 031305.
[6] Szymanski K. and Labaye Y., *Phys. Rev. E*, **59** (1999) 2863.
[7] Nakamura K., Kurosawa M. and Ueha S., *IEEE Trans. UFFC*, **40** (1993) 395.
[8] Wajchman D., Liu K.-C., Friend J. and Yeo L., *IEEE Trans. UFFC*, **55** (2008) 832.
[9] Online videos of multiple-toss, accessed 29 April, 2008: `http://www.throwdough.com/trick_basictoss.htm` and `http://www.youtube.com/watch?v=fAW0aDWaiSI`.
[10] Hu J., Nakamura K. and Ueha S., *Ultrasonics*, **35** (1997) 459.
[11] Ide T., Friend J., Nakamura K. and Ueha S., *Sens. Actuators A: Phys.*, **135** (2007) 740.
[12] Saito J., Friend J., Nakamura K. and Ueha S., *Jpn. J. Appl. Phys.*, **44** (2005) 4666.
[13] Nusse H. L. and Yorke J. A., *Dynamics: Numerical Explorations* (Springer-Verlag) 1994.